Thermodynamics of Sublimation, Crystal Lattice Energies, and Crystal Structures of Racemates and Enantiomers: (+)- and (±)-Ibuprofen

GERMAN L. PERLOVICH,[1,2] SERGEY V. KURKOV,[2] LARS KR. HANSEN,[3] ANNETTE BAUER-BRANDL[1]

[1]University of Tromsø, Institute of Pharmacy, Breivika, N-9037 Tromsø, Norway

[2]Institute of Solution Chemistry, Russian Academy of Sciences, 153045 Ivanovo, Russia

[3]University of Tromsø, Institute of Chemistry, Breivika, N-9037 Tromsø, Norway

Received 30 April 2003; revised 20 September 2003; accepted 2 October 2003

ABSTRACT: Thermodynamic differences between ibuprofen (IBP) racemate and the (+)-enantiomer were studied by X-ray diffraction, thermoanalysis, and crystal energy calculations. The thermodynamic functions of sublimation (as a measure of crystal lattice energy) were obtained by the transpiration method. The sublimation enthalpies (ΔH_{sub}) of (±)-IBP and (+)-IBP are 115.8 ± 0.6 and 107.4 ± 0.5 kJ · mol^{-1}, respectively. Using the temperature dependency of the saturated vapor pressure, the relative fractions of enthalpy and entropy of the sublimation process were calculated, and the sublimation process for both the racemate and the enantiomer was found to be enthalpy driven (62%). Two different force fields, Mayo et al. (**M**) and Gavezzotti (**G**), were used for comparative analysis of crystal lattice energies. Both force fields revealed that the van der Waals term contributes more to the packing energy in (+)-IBP than in (±)-IBP. The hydrogen bonding energy, however, contributes at 29.7 and 32.3% to the total crystal lattice energy in (+)-IBP and (±)-IBP (**M**), respectively. Furthermore, different structure fragments of the IBP molecule were analyzed with respect to their contribution to nonbonded van der Waals interactions. The effect of the C–H distance on the van der Waals term of the crystal lattice energy was also studied. J Pharm Sci 93:654–666, 2004

Keywords: (+)-ibuprofen; (±)-ibuprofen; chirality; thermodynamics; crystallography; thermal analysis; crystal structure

INTRODUCTION

Chemistry of life is essentially chiral, and stereochemistry is inherent in all biochemical processes, affecting the whole spectrum of pharmaceutical, agricultural, cosmetics, and nutrition industries.[1] Enantiomers of chiral drugs may differ considerably in their pharmacological and toxicological effects because they interact with biological macromolecules, which are stereoselective.[2] Furthermore, there can be considerable differences in the solid material properties, which are of importance for handling, production, and performance of drug preparations. X-ray analysis (see, for example, Ref. 3) and differential scanning calorimetry (DSC)[4] are commonly used methods for studying differences in physicochemical properties between homochiral and heterochiral materials. However, because of the considerable difficulties connected with practical experiments and their interpretation, computer modeling has been introduced in recent years as an additional method for a better understanding of chirality.[4–6]

Correspondence to: Annette Bauer-Brandl (Telephone: 47 77646160; Fax: 47 77646151;
E-mail: annetteb@farmasi.uit.no)

Journal of Pharmaceutical Sciences, Vol. 93, 654–666 (2004)

Crystal structure data are important to describe and interpret the particularities of chiral compounds. Pure enantiomers form crystals in chiral space groups (with a limited number of elements of symmetry). Racemic compounds, however, have a wider choice of elements of symmetry and can crystallize in one of the centrosymmetric space groups.[3] Furthermore, the network of hydrogen bonds plays an important role in determining the architecture of the crystals. Hydrogen bonds are characterized by specific geometric and energetic properties and contribute considerably to the packing energy. Hydrogen bonds of homochiral and of racemic crystals have their respective unique characteristics and may essentially influence the thermodynamics and kinetics of crystal growth.[4,5,7] A better understanding of the intermolecular interactions associated with the recognition or discrimination of a chiral molecule while crystallization takes place may enable enantioselective crystallization and, consequently, optimum drug design.

In the present study, detailed investigations of thermodynamic and energetic aspects of the sublimation process of (+)- and (±)-ibuprofen (IBP)—as a representative of nonsteroidal antiinflammatory drugs—were carried out. In the case of IBP, it is not the pharmacological performance that is of outstanding interest in drug design: although the *S*(+) enantiomer of IBP is the only pharmacologically active molecule, the racemate is almost as active *in vivo* because the *S*(+) enantiomer is continuously formed metabolically from *R*(−)-IBP.[25,27] IBP is particularly interesting with respect to chirality for the following reasons: First, the explicit structures of both (+)- and (±)-IBP crystals have already been solved by various diffraction methods, like X-ray[8,9] and pulsed neutron diffraction.[5,10] Second, (±)-IBP is one of the very rare examples of drug substances for which thermodynamic data of sublimation have been published.[11] Third, experimental thermochemical data on the melting process both of the (+)-enantiomer[4,20] and the racemate[12,20] are also available. These data will be useful in interpretation of the present data.

EXPERIMENTAL

Materials and Solvents

(+)-Ibuprofen [(+)-IBP; *S*(+)-2-(4-isobutylphenyl) propionic acid, $C_{13}H_{18}O_2$; MW, 206.3; $[\alpha]_{546}^{20} = 58 \pm 3^{\circ}$; puriss ≥99.0%] was purchased from Fluka (Lot 357891/1). (±)-Ibuprofen [(±)- IBP; (±)-2-(4-isobutylphenyl)propionic acid; puriss ≥99.7%) was purchased from Sigma (Lot 26H1368).

Sublimation Experiments

Sublimation experiments were carried out by the transpiration method as described elsewhere.[13] In brief, a stream of an inert gas is passed above the sample at a constant temperature and at a known slow constant flow rate to achieve saturation of the carrier gas with the vapor of the substance under investigation. The vapor is condensed at some point downstream, and the mass of sublimate and its purity are determined. The amount of sublimated substance is determined by dissolving the condensed substance in a defined volume of solvent (V_{sol}). The mass of the substance is quantified sprectroscopically by determining the absorbance, *A*, of the solution with a Hitachi spectrophotometer (model U-2001). In these experiments, the solvent was ethyl alcohol and the absorbance was measured at 220 nm.

The sublimation device was tested before starting the experiments by determining the relation between *P* and ν and choosing the gas flow velocity value within the plateau of the $P = f(\nu)$ curve. The velocity of carrier gas flow for the considered compounds was 1.8 dm^3/h. The equipment was calibrated with benzoic acid (standard substance obtained from Polish Committee of Quality and Standards), which has an enthalpy of combustion (ΔH_c) of $-3228.07\ kJ \cdot mol^{-1}$ and a heat of melting (ΔH_{fus}) of $18.0\ kJ \cdot mol^{-1}$. The standard value of sublimation enthalpy (ΔH^0_{sub}) obtained here was $90.5 \pm 0.3\ J \cdot mol^{-1}$. This value is in good agreement with the ΔH^0_{sub} of $89.7 \pm 0.5\ J \cdot mol^{-1}$ recommended by IUPAC.[14] The saturated vapor pressures were measured five times at each temperature, and the standard deviation was within 3–5%. The experimentally determined vapor pressure data were described in (ln *P*;1/*T*) coordinates by eq. 1:

$$\ln P = A + B/T \quad (1)$$

The value of the enthalpy of sublimation was calculated by the Clausius–Clapeyron equation

$$\Delta H^{T}_{sub} = -RT^2 \cdot \partial(\ln P)/\partial(T) \quad (2)$$

The entropy of sublimation at a given temperature *T* was calculated from the following relation:

$$\Delta S^{T}_{sub} = (\Delta H^{T}_{sub} - \Delta G^{T}_{sub})/T \quad (3)$$

where $\Delta G^{T}_{sub} = -RT \cdot \ln(P/P_0)$ and $P_0 = 1.013 \cdot 10^5$ Pa.

Energy Calculation Procedure

Molecular crystals consist of discrete molecules that interact with each other by intermolecular nonbonded interactions. Therefore, the crystal lattice energy, E_{latt}, may conditionally be divided into three main terms: van der Waals, E^{vdw}, electrostatic (Coulombic), E^{coul}, and hydrogen bonds energy, E^{HB}

$$E_{\text{latt}} = E^{\text{vdw}} + E^{\text{coul}} + E^{\text{HB}} \quad (4)$$

Nonbonded van der Waals interactions of the crystal lattice energy have been calculated as the sum of atom−atom interactions.[15] The cut-off radius was chosen as 16 Å because the calculated E^{vdw} values were 99% of common E^{vdw}. The choice of the potential function used for the pairwise calculation is important for the value of the van der Waals term. Two types of the force fields are common: Mayo et al.[16] (Lenard−Jones 12-6) (**M**) and Gavezzotti[17] (exponential-6 form) (**G**). In the present study, both types were used and compared.

A Coulomb potential with atom-centered point charges was used to describe the electrostatic interactions. It should be noted, that the calculation of this term is problematic for ionic compounds because it is difficult to determine the coordinates of point charges. Because of this difficulty, some authors (see for example, Gavezzotti et al.[17]) include electrostatic terms in van der Waals terms, with slightly different equilibrium distances between nonbonded atoms. Because the noted moments are questionable, we tried to compare the two approaches with the two types of force fields **G** and **M** already mentioned. The standard software HyperChem, release 5.02 (semi-empiric method PM3) was used to calculate the point charges of the atoms. As a first approximation, the point charges were obtained by the "single point" option for single molecules in vacuum, having the same conformational state as in the crystal lattice.

The hydrogen bonding energy was also calculated by the same potentials **M** and **G**. It should be noted, that the approach of Mayo et al.[16] allows one to obtain E^{HB} without knowledge of the hydrogen atoms coordinates, whereas the calculation procedure of Gavezzotti[17] strongly depends on these parameters.

X-ray Diffraction Measurements

Single-crystal X-ray measurements were carried with a Nonius CAD-4 diffractometer with graphite-monochromated Mo K_α radiation ($\lambda = 0.71069$ Å). Intensity data were collected at 25°C with a ω-2θ scanning procedure up to $2\theta = 54°$. The crystal structure was solved by direct methods and refined by a full-matrix least-squares procedure. All programs used for the solution, refinement, and display of the structures are included in the *OSCAIL* program package.[22] *CAD-4* Software[23] was used for data collection, data reduction, and cell refinement. Programs *SHELXS-97*[22] and *SHELXL-97*[24] were used to solve and to refine structures, respectively.

RESULTS AND DISCUSSION

(+)- and (±)-Ibuprofen Crystal Structures

Before discussing thermodynamic characteristics of (+)- and (±)-IBP, a detailed description of their crystal structures is needed. (±)-IBP has been solved by two different methods: X-ray diffraction at room temperature (10−30°C) by McConnell[9] (refcode in Cambridge Structural Database, CSD, CSD−IBPRAC) and single-crystal pulsed-neutron diffraction at −173°C by Shankland et al.[10] (refcode CSD−IBPRAC02). The structure of (+)-IBP was solved by the X-ray diffraction method at room temperature (10−30°C) by Freer et al.[8] (refcode CSD−JECNOC 10), but only for heavy atoms. The latter fact limits the quality of estimation of the crystal lattice energy (especially the hydrogen bond energy). Therefore, to carry out a new X-ray diffraction experiment, (+)-IBP single crystals were grown from a saturated solution in *n*-heptanol by slow evaporation. The X-ray diffraction experiment was carried out at 25°C with a complete (total) refinement of both the heavy and the hydrogen atoms. The results of the experiment are presented in Table 1 together with analogous values for the racemate obtained by Shankland et al.[10] (which are used to estimate the crystal lattice energy thereof). It should be mentioned that the data of Shankland et al.[10] were chosen because the neutron diffraction experiment gives a more precise determination of the coordinates of the hydrogen atoms than does the X-ray diffraction method. Unfortunately, we had no opportunity to carry out a neutron diffraction experiment with the noted enantiomer crystal. Therefore, in the calculation part of the present work, we analyzed the influence of varying C−H distances on the results of the calculation (as is usually done in the same situations[15]).

Table 1. Crystal Lattice Parameters of (±)- and (+)-Ibuprofen[a]

Parameter Crystal Data	(±)-IBP Shankland et al.[b]	(+)-IBP This Work
Crystal system	Monoclinic	Monoclinic
Space group	$P2_1/c$	$P2_1$
Description	Rectangular plate	Colorless block
Crystal size, mm	$5.0 \times 2.0 \times 1.0$	$0.40 \times 0.40 \times 0.30$
a, Å	14.397 (8)	12.456 (4)
b, Å	7.818 (4)	8.0362 (11)
c, Å	10.506 (6)	13.533 (3)
β, °	99.70 (3)	112.86 (2)
Volume, Å^3	1165.6 (11)	1248.2 (5)
Z	4	4
D_{calc}, g · cm^{-3}	1.175	1.098
Radiation[c]	Pulsed neutron	Mo K_α
T, °C	−173	25 (2)
μ, mm^{-1}		0.072
Data collection		
Measured reflections	8085	3086
Independent reflections	1528	2910
Independent reflections with $> 2\sigma(I)$	1449	1683
R_{int}	0.06	0.0118
θ_{max}, °		26.96
Refinement		
Refinement on	F	F^2
$R[F^2 > 2\sigma(F^2)$	0.077	0.0385
$\omega R(F^2)$	0.053	0.1050
S	1.76	0.982
Reflections	1449	2910
Parameters	298	416
$(\Delta/\sigma)_{max}$	0.03	0.002
Δ_{max}, e · Å^{-3}		0.119
Δ_{min}, e · Å^{-3}		−0.113
Extinction correction		SHELXL[d]
Extinction coefficient	0.05 (1)	0.016 (3)

[a]Standard deviations displayed in parentheses.
[b](CSD-IBPRAC02) from Ref. 10.
[c]Pulsed neutron (λ = 0.48–4.8 Å); Mo K_α (λ = 0.71069 Å).
[d]Reference 24.

The fractional atomic coordinates and equivalent isotropic displacement parameters of (+)-IBP are presented in Table 2. Two molecules in both of the crystal lattices of (+)- and of (±)-IBP form a cyclic dimer through hydrogen bonds of their carboxylic groups. However, in the unit cell of (+)-IBP, both molecules are in the *S-configuration*, and they are in different conformational states (Fig. 1a). In contrast, the (±)-IBP dimer is formed by hydrogen bonds across a center of inversion (space group $P2_1/c$), with one molecule in the *R*-configuration and the other in the *S*-configuration (Fig. 1b).

A similar analysis of conformational states of the molecules of (+)- and (±)-IBP in the respective crystal lattices was carried out in detail by Freer et al.[8] Another study to consider is that of Shankland et al.,[21] in which possible reasons for the distortion of the IBP molecular skeleton in the crystal lattices in comparison to the gas phase were studied. In this study, the (+)-IBP structure has been refined, not only with respect to the heavy atoms but also with respect to the hydrogen atoms. Some special characteristics of the conformational states and the geometry of hydrogen bonds of both (+)- and (±)-IBP are presented in Table 3. Because the two molecules of (+)-IBP are situated in the asymmetric unit, the geometries of the two hydrogen bonds are not equivalent; that is, one of them is shorter than the other. Comparison of the data leads to the following conclusions: (a) the angle of the hydrogen bonding of the racemate

Table 2. Fractional Atomic Coordinates and Equivalent Isotropic Displacement Parameters of (+)-Ibuprofen

Atom	X/a	y/b	z/c	$U_{eq}{}^{a}$
O1A	0.4640 (2)	−0.0661 (4)	−0.2241 (2)	0.0890 (8)
O2A	0.58499 (19)	−0.2352 (3)	− 0.10390 (18)	0.0757 (6)
C1A	0.4879 (3)	−0.2052 (4)	−0.1705 (2)	0.0613 (8)
C2A	0.3900 (3)	−0.3274 (4)	−0.1995 (3)	0.0680 (9)
C3A	0.4028 (4)	−0.4412 (7)	−0.1044 (4)	0.0899 (13)
C4A	0.3837 (2)	−0.4215 (4)	−0.2990 (2)	0.0592 (8)
C5A	0.3135 (3)	−0.3645 (5)	−0.4000 (3)	0.0776 (10)
C6A	0.3095 (3)	−0.4468 (5)	−0.4913 (3)	0.0795 (10)
C7A	0.3752 (3)	−0.5870 (4)	−0.4856 (3)	0.0666 (9)
C8A	0.4460 (3)	−0.6415 (5)	−0.3850 (3)	0.0685 (9)
C9A	0.4501 (3)	−0.5605 (4)	−0.2941 (3)	0.0659 (9)
C10A	0.3649 (4)	−0.6796 (6)	−0.5864 (3)	0.0820 (12)
C11A	0.2651 (3)	−0.8032 (5)	−0.6258 (3)	0.0756 (10)
C13A	0.2856 (5)	−0.9476 (6)	−0.5496 (4)	0.0920 (13)
C12A	0.2441 (5)	−0.8664 (9)	−0.7376 (3)	0.1028 (14)
O1B	0.7685 (2)	−0.0391 (3)	−0.04780 (18)	0.0710 (6)
O2B	0.6486 (2)	0.1313 (3)	−0.16958 (17)	0.0840 (7)
C1B	0.7446 (3)	0.1014 (4)	−0.0998 (2)	0.0547 (7)
C2B	0.8429 (3)	0.2278 (4)	−0.0655 (2)	0.0590 (8)
C3B	0.9591 (3)	0.1463 (6)	−0.0477 (4)	0.0835 (11)
C4B	0.8401 (2)	0.3199 (3)	0.0314 (2)	0.0497 (7)
C5B	0.9085 (3)	0.2746 (4)	0.1358 (2)	0.0599 (8)
C6B	0.9054 (3)	0.3626 (4)	0.2220 (2)	0.0604 (8)
C7B	0.8336 (2)	0.4998 (3)	0.2083 (2)	0.0493 (7)
C8B	0.7632 (2)	0.5422 (4)	0.1041 (2)	0.0548 (7)
C9B	0.7668 (2)	0.4546 (4)	0.0175 (2)	0.0547 (7)
C10B	0.8355 (3)	0.5965 (4)	0.3034 (2)	0.0614 (8)
C11B	0.9402 (3)	0.7128 (5)	0.3508 (2)	0.0688 (9)
C12B	0.9347 (5)	0.8545 (7)	0.2759 (4)	0.1068 (17)
C13B	0.9486 (6)	0.7781 (7)	0.4595 (4)	0.1045 (15)
H1AO	0.533 (4)	−0.007 (8)	−0.208 (4)	0.16 (2)
H3A1	0.481 (4)	−0.502 (6)	−0.073 (3)	0.131 (16)
H3A2	0.403 (3)	−0.385 (6)	−0.050 (3)	0.104 (14)
H3A3	0.332 (3)	−0.522 (6)	−0.127 (3)	0.108 (12)
H2A	0.326 (3)	−0.265 (5)	−0.217 (3)	0.096 (12)
H5A	0.271 (3)	−0.283 (5)	−0.398 (2)	0.074 (10)
H6A	0.257 (3)	−0.404 (6)	−0.563 (3)	0.105 (12)
H8A	0.500 (3)	−0.738 (5)	−0.376 (2)	0.074 (9)
H9A	0.500 (3)	−0.598 (4)	−0.227 (3)	0.058 (8)
H11A	0.195 (4)	−0.741 (6)	−0.642 (3)	0.111 (14)
H101	0.434 (3)	−0.741 (5)	−0.577 (3)	0.088 (12)
H102	0.348 (3)	−0.600 (6)	−0.645 (3)	0.115 (15)
H121	0.298 (3)	−0.904 (6)	−0.474 (3)	0.108 (12)
H122	0.210 (4)	−1.024 (7)	−0.584 (3)	0.122 (14)
H1BO	0.688 (4)	−0.106 (6)	−0.077 (3)	0.113 (13)
H2B	0.821 (2)	0.309 (4)	−0.128 (2)	0.064 (8)
H5B	0.966 (2)	0.183 (4)	0.152 (2)	0.071 (9)
H6B	0.957 (3)	0.326 (4)	0.298 (3)	0.075 (10)
H8B	0.712 (3)	0.632 (5)	0.093 (2)	0.073 (9)
H9B	0.712 (3)	0.480 (5)	−0.053 (3)	0.093 (11)
H11B	1.020 (3)	0.655 (4)	0.3544 (19)	0.065 (8)
H3B1	1.020 (4)	0.236 (8)	−0.031 (4)	0.144 (18)
H3B2	0.949 (2)	0.094 (4)	−0.118 (2)	0.072 (9)

(*Continued*)

Table 2. (*Continued*)

Atom	X/a	y/b	z/c	U_{eq}[a]
H3B3	0.990 (3)	0.047 (6)	0.017 (3)	0.117 (14)
H133	0.170 (5)	−0.953 (8)	−0.765 (4)	0.16 (2)
H123	0.363 (5)	−1.006 (10)	−0.537 (4)	0.19 (3)
H132	0.225 (4)	−0.765 (7)	−0.783 (4)	0.129 (18)
H131	0.328 (4)	−0.925 (7)	−0.732 (4)	0.16 (2)
H126	0.865 (6)	0.933 (12)	0.286 (6)	0.24 (4)
H125	0.913 (4)	0.826 (6)	0.200 (4)	0.114 (14)
H124	1.015 (5)	0.917 (9)	0.310 (4)	0.16 (2)
H103	0.840 (2)	0.513 (4)	0.360 (2)	0.068 (9)
H104	0.761 (3)	0.665 (4)	0.279 (2)	0.065 (9)
H136	0.883 (4)	0.850 (7)	0.435 (4)	0.14 (2)
H134	1.009 (3)	0.841 (5)	0.486 (3)	0.074 (11)
H135	0.949 (5)	0.679 (10)	0.516 (5)	0.19 (3)

[a] $U_{eq} = (1/3) \cdot \sum_i \sum_j U^{ij}\, a^i \cdot a^j\, \mathbf{a}_i \cdot \mathbf{a}_j$.

is more planar than that of the enantiomer; (b) the D...A distance of one of the hydrogen bonds of the (+)-IBP is approximately equal (within experimental errors) to the analogous value of the enantiomer, whereas the second hydrogen bond is longer; and (c) the H...A distance of the (+)-IBP is the average of the analogous values of the enantiomer. The conformational states of the enantiomer molecules in the asymmetric unit cell are different. As shown in Table 3, one of the two molecules in the (+)-IBP asymmetric cell has approximately the same conformational state as in the racemic IBP crystal.

Thermodynamics of (+)- and (±)-IBP Sublimation

The temperature dependencies of the saturation vapor pressure as well as the thermodynamic sublimation functions for (+)- and (±)-IBP are presented in Table 4. The temperature interval for the measurement of saturation vapor pressures of (+)- and racemic-IBP was chosen on the basis of optimum conditions in terms of minimum experimental error of the method used. The upper limit of the experiments for (+)-IBP was determined by the melting point of the compound: $T_m = 50.3 \pm 0.4$°C (Table 5). At temperatures

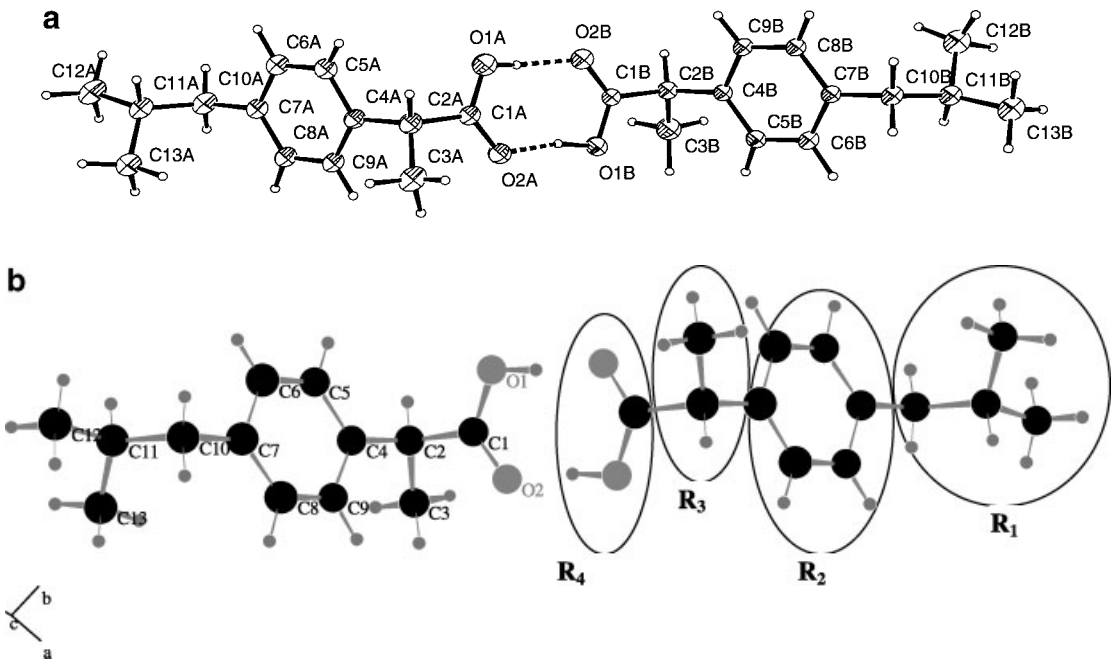

Figure 1. A perspective view of the cyclic dimer of (a) (+)-ibuprofen and (b) (±)-ibuprofen (fragmentation of the molecule for calculations).

Table 3. Parameters that Characterize the Conformational States and Hydrogen Bond Geometry of (+)- and of (±)-Ibuprofen Molecules in the Crystal Lattice

	(+)-IBP		
Parameter	A	B	(±)-IBP[a]
∠C5–C4–C2–C3 (°)	144.4 (4)	−29.1 (4)	140.9 (4)
∠C7–C10–C11–C12 (°)	−67.9 (5)	68.0 (5)	−67.3 (4)
∠C4–C2–C1–O1 (°)	81.7 (4)	−83.5 (3)	88.7 (3)
O2–C1 (Å)	1.219 (3)	1.226 (3)	1.222 (3)
O1–C1 (Å)	1.302 (4)	1.302 (4)	1.305 (3)
C1–C2 (Å)	1.496 (5)	1.518 (4)	1.509 (3)

Hydrogen bond geometry

Molecule	D–H...A	D–H (Å)	H...A (Å)	D...A (Å)	D–H...A (°)
(+)-IBP (A)	O1A-H1AO...O2B	0.94 (5)	1.73 (6)	2.651 (4)	169 (5)
(+)-IBP (B)	O1B-H1BO...O2A	1.07 (5)	1.58 (5)	2.634 (4)	168 (4)
(±)-IBP[a]	O1-H1O...O2[b]	0.963 (13)	1.664 (10)	2.627 (7)	179.5 (7)

[a]Reference 10.
[b]Symmetry code: $1-x, 1-y, 1-z$.

Table 4. Temperature Dependence of Saturation Vapor Pressure and the Sublimation Thermodynamic Functions of (±)-Ibuprofen and (+)-Ibuprofen

(±)-IBP		(+)-IBP	
t (°C)	P (Pa)	t (°C)	P (Pa)
40	$1.66 \cdot 10^{-2}$	32	$1.40 \cdot 10^{-2}$
43	$2.55 \cdot 10^{-2}$	33	$1.59 \cdot 10^{-2}$
45	$3.44 \cdot 10^{-2}$	34	$1.81 \cdot 10^{-2}$
46	$4.00 \cdot 10^{-2}$	35	$2.13 \cdot 10^{-2}$
47	$4.42 \cdot 10^{-2}$	36	$2.42 \cdot 10^{-2}$
48	$4.98 \cdot 10^{-2}$	37	$2.73 \cdot 10^{-2}$
49	$5.84 \cdot 10^{-2}$	38	$3.17 \cdot 10^{-2}$
50	$6.86 \cdot 10^{-2}$	39	$3.62 \cdot 10^{-2}$
51	$7.35 \cdot 10^{-2}$	40	$4.16 \cdot 10^{-2}$
52	$8.13 \cdot 10^{-2}$	41	$4.74 \cdot 10^{-2}$
53	$9.63 \cdot 10^{-2}$	42	$5.34 \cdot 10^{-2}$
54	$1.15 \cdot 10^{-1}$	43	$6.02 \cdot 10^{-2}$
55	$1.22 \cdot 10^{-1}$	44	$6.93 \cdot 10^{-2}$
56	$1.42 \cdot 10^{-1}$	45	$7.81 \cdot 10^{-2}$
57	$1.64 \cdot 10^{-1}$		
58	$1.90 \cdot 10^{-1}$		
59	$2.10 \cdot 10^{-1}$		
60	$2.39 \cdot 10^{-1}$		
61	$2.78 \cdot 10^{-1}$		
62	$3.17 \cdot 10^{-1}$		
63	$3.57 \cdot 10^{-1}$		
64	$4.11 \cdot 10^{-1}$		
65	$4.40 \cdot 10^{-1}$		
66	$5.04 \cdot 10^{-1}$		
67	$5.64 \cdot 10^{-1}$		
$\ln(P[\text{Pa}]) = (40.4 \pm 0.2) - (13927 \pm 73)/T$		$\ln(P[\text{Pa}]) = (38.1 \pm 0.2) - (12920 \pm 60)/T$	
$r = 0.999$; $\sigma = 2.54 \cdot 10^{-2}$; F = 36648; $n = 25$		$r = 0.999$; $\sigma = 9.1 \cdot 10^{-3}$; F = 48662; $n = 14$	

<50.3°C, the vapor pressure of the racemate is much lower than that of (+)-IBP because of its higher crystal lattice energy. This fact is an essential obstacle to obtaining P values with comparable experimental errors. The lowest temperature at which the experimental errors for both the racemate and the enantiomer are still comparable, 40°C, was therefore set as the lowest experimental temperature. However, the obtained set of experimental data points ($n = 25$ for racemate-IBP and $n = 14$ for the enantiomer) enable (a) interpolation (and extrapolation to 25°C) of the function $\ln(P) = f(1/T)$; (b) calculation of all thermodynamic functions; and (c) correct comparison of the experimental data and the functions with each other. There are three distinct temperatures within the interval at which vapor pressure data for both the racemate and the enantiomer are available (i.e., $T = 40$, 43, or 45°C), once more confirming the validity of this procedure.

The saturation vapor pressure of the (+)-IBP enantiomer is higher than that for the racemate (at the same temperature), and the sublimation enthalpy of the enantiomer is lower by 8.4 $\text{kJ} \cdot \text{mol}^{-1}$ compared with that of the racemate. (±)-IBP is one of the rare examples in which the temperature dependence of saturation vapor pressures of a drug substance has been previously published. The experimental data of Ertel et al.[11] and the present study are compared in Figure 2. The values of saturation vapor pressures obtained by Ertel et al. by the effusion method and those obtained in the present work by the transpiration method are quite close to each other.[11] However, there is a

Table 5. Thermochemical Characteristics of (+)- and (±)-Ibuprofen

Parameter	(±)-IBP	(+)-IBP	Δ((±) − (+))
ΔG_{sub}^{298} (kJ · mol^{-1})	44.2	41.6	2.6
ΔH_{sub}^{298} (kJ · mol^{-1})	115.8 ± 0.6	107.8 ± 0.5	8.4
$T \cdot \Delta S_{sub}^{298}$ (kJ · mol^{-1})	71.6	65.8	5.8
ΔS_{sub}^{298} (J · mol^{-1} · K^{-1})	240 ± 2	221 ± 2	19
ε_H (%)[a]	61.8	62.0	−0.2
ε_{TS} (%)[a]	38.2	38.0	0.2
T^f (°C)	74.0 ± 0.4[b]	50.3 ± 0.4[c]	23.7
ΔH_{fus} (kJ · mol^{-1})	23.1 ± 0.4[b]	15.4 ± 0.4[c]	7.7
ΔH_{fus} (kJ · mol^{-1})[d]	25.5	17.9	7.6
ΔS_{fus} (J · mol^{-1} · K^{-1})[e]	67	48	19
ΔS_{fus} (J · mol^{-1} · K^{-1})[d]	73.2	54.8	18.4
ΔH_{vap} (kJ · mol^{-1})	92.7	92.0	0.7
ΔS_{vap} (J · mol^{-1} · K^{-1})	173	173	0

[a] $\varepsilon_H = (\Delta H_{sub}^{298}/(\Delta H_{sub}^{298} + T \cdot \Delta S_{sub}^{298})) \cdot 100\%$; $\varepsilon_{TS} = (T \cdot \Delta S_{sub}^{298}/(\Delta H_{sub}^{298} + T \cdot \Delta S_{sub}^{298})) \cdot 100\%$.
[b] Reference 12.
[c] Reference 4.
[d] Reference 20.
[e] $\Delta S_{fus} = \Delta H_{fus}/T^f$.

considerable difference between the sublimation enthalpy values extrapolated to room temperature: 115.8 ± 0.6 (this work) compared with 121 ± 2 kJ · mol^{-1} (Ertel et al.[11]). This difference may be explained as follows: Ertel et al.[11] obtained data from two series of experiments in which two different geometries of effusion cells were used: "high temperature" (47–64°C, 7 experimental data points, with the diameter of the effusion orifice being 0.2580 cm), and "low temperature" (23–45°C, 8 experimental points, with the effusion orifice diameter of 0.0592 cm). If one calculates ΔH_{sub} for their "high temperature" region separately, the value 117 ± 2 kJ · mol^{-1} is derived, whereas the analogous value for their "low temperature" region is 124 ± 2 kJ · mol^{-1}. It is obvious that the ΔH_{sub} value of the "high temperature" region corresponds (within experimental error) very well with the ΔH_{sub} value of the present study in which a different method of measurement was used. This finding may indicate that the effusion method used by Ertel et al.[11] could be sensitive to the effusion cell geometry (orifice area) and to the calibration procedure, and therefore, reference substances that are structurally related to the substance under investigation may be necessary.

Absorption spectra and extinction coefficients of the initial material, of the material remaining in the sample chamber after the experiment, and of the sublimate (downstream) were measured and compared. The absorption spectra and extinction coefficients coincided within experimental error. Additionally, thin-layer chromatography (TLC) was used for each noted fraction. The results did not show any traces of the decomposition product. Furthermore, the vapor pressure values for (±)-IBP of the present study are in good agreement with analogous values obtained by Ertel et al.[11] in the same temperature interval using another method. Ertel et al. also did not observe any decomposition of the compound.[11] All the arguments mentioned suggest that the present experimental results are accurate enough to describe the sublimation process correctly.

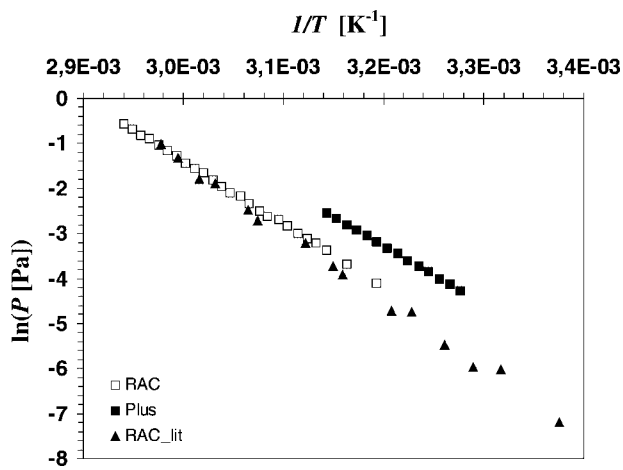

Figure 2. Temperature dependence of a saturated vapor pressure of (±)-ibuprofen [□, RAC (this work) and (▲) RAC_lit (from ref 11)] and (+)-ibuprofen (■, Plus).

Thermodynamic parameters of sublimation and other thermoanalytical characteristics for (±)- and (+)-IBP are presented in Table 5. The difference between the enthalpies of fusion (7.7 $kJ \cdot mol^{-1}$) corresponds to the difference between the ΔH_{sub} values (8.4 $kJ \cdot mol^{-1}$) within experimental errors. This similarity indicates that the interactions between molecules in the liquid state of both the racemate and the pure enantiomer are energetically equal.

The Gibbs energy of the sublimation process at room temperature of (±)- and (+)-IBP can be separated into the relative fractions of both the enthalpic and the entropic terms by the following parameters:

$$\varepsilon_H = \left(\Delta H^{298}_{sub} / \left(\Delta H^{298}_{sub} + T \cdot \Delta S^{298}_{sub}\right)\right) \cdot 100\% \quad (5)$$

$$\varepsilon_{TS} = \left(T \cdot \Delta S^{298}_{sub} / \left(\Delta H^{298}_{sub} + T \cdot \Delta S^{298}_{sub}\right)\right) \cdot 100\% \quad (6)$$

Results of these calculations are also shown in Table 5. The sublimation process, for both the racemate and the enantiomer, consists of 62% enthalpy and 38% entropy. Approximately equal values are found when the same calculations are carried out for a structurally related molecule [namely, benzoic acid (BA)], using literature values,[13] (i.e., $\varepsilon_H = 61.7\%$, and $\varepsilon_{TS} = 38.3\%$).

Biphenyl derivatives of carbonic acids, diflunisal (DIF), and flurbiprofen (FBP)[18] are structurally more complicated substances of the same group of nonsteroidal antiinflammatory drugs. The respective values for diflunisal are $\varepsilon_H(DIF) = 65.9\%$ and $\varepsilon_{TS}(DIF) = 34.1\%$, and those for flurbiprofen are $\varepsilon_H(FBP) = 66.3\%$ and $\varepsilon_{TS}(FBP) = 33.7\%$. These values are close to each other. However, in comparison with IBP and BA, the enthalpic terms of DIF and FBP increase by ~4%. In all cases, enthalpy exceeds entropy.

Also, for comparison reasons, benzene and biphenyl as the nonsubstituted analogues of the noted molecules (which in the crystal lattice only interact nonspecifically by van der Waals forces) were investigated.[19] The values of enthalpy and entropy for the solid state of benzene differ significantly from the substances already considered [$\varepsilon_H(Ben) = 52.5\%$, $\varepsilon_{TS}(Ben) = 47.5\%$], whereas the analogous values of biphenyl are close to those of BA and IBP [i.e., $\varepsilon_H(BiPh) = 59.9\%$, $\varepsilon_{TS}(BiPh) = 40.1\%$]. The explanation for this nonsystematic sharing between enthalpy and entropy with respect to the skeletal structures is supposed to be a different distribution of the total crystal lattice energy between van der Waals interactions and hydrogen bonds depending on the functional groups in the molecules.

It is interesting to note that the difference between the Gibbs energies of (±)- and (+)-IBP at 25°C is 2.6 $kJ \cdot mol^{-1}$ (Table 5). This value practically coincides with the value of heat fluctuation, $RT = 2.5$ $kJ \cdot mol^{-1}$. This fact once more confirms that the problem of separation of the enantiomers is very delicate. Using the thermodynamic cycle (while neglecting the differences of the heat capacities between the racemate and chiral substances, which is supposed to be very small), the thermodynamic functions of evaporation of both (±)- and (+)-IBP may be estimated as follows:

$$\Delta H_{vap} = \Delta H_{sub} - \Delta H_{fus} \quad (7)$$

$$\Delta S_{vap} = \Delta S_{sub} - \Delta S_{fus} \quad (8)$$

The values are given in Table 5. Enthalpies of evaporation, ΔH_{vap}, of both the enantiomer and the racemate coincide at 92 $kJ \cdot mol^{-1}$ because the differences in ΔH_{sub} for the enantiomer and the racemate (measured in the present paper) and of ΔH_{fus} (enantiomer[20] and racemate[12]) are equal. The standard value of entropy of sublimation of (±)-IBP exceeds that of (+)-IBP by 19 $J \cdot mol^{-1} \cdot K^{-1}$. The difference between the entropies of fusion between the racemate and the enantiomer is also 19 $J \cdot mol^{-1} \cdot K^{-1}$ (Table 5). Therefore, the entropy of evaporation for both considered compounds coincides at 173 $J \cdot mol^{-1} \cdot K^{-1}$. These facts indicate that the respective experimental data both from the cited literature and the present paper are accurate (within experimental error).

Based on the thermodynamic cycle (Fig. 3), the difference between the entropies of (±)- and (+)-IBP crystal lattices may be calculated as:

$$\Delta\Delta S = \Delta S_{sub}(\pm) - \Delta S_{sub}(+) - R \ln 2 = 13.1 \text{ J} \cdot \text{mol}^{-1} \cdot \text{K}^{-1} \quad (9)$$

This value quantifies the difference between the entropies of the crystal lattices of the racemate and the enantiomer, which is caused only by particularities of the respective crystal lattice structures. In the following discussion this difference will be investigated with respect to the contribution of various energetic terms to the crystal lattice energies for both (±)- and (+)-IBP.

Calculation Results of the Crystal Lattice Packing Energies

For a deeper understanding of the nature of interaction of IBP molecules both in the racemate

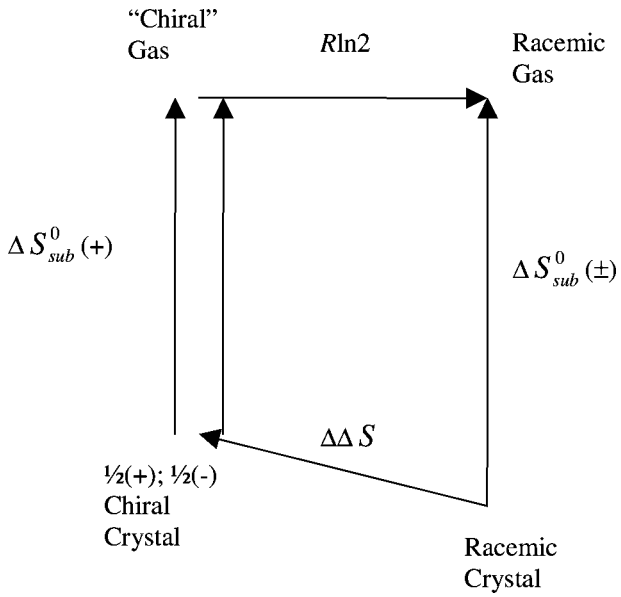

Figure 3. Thermodynamic cycle for the racemate and enantiomer crystals.

and the enantiomer in the crystal lattice, the packing energies were calculated. For this purpose X-ray data for (+)-IBP obtained in this work and the neutron diffraction data for (±)-IBP from Shankland et al.[10] (refcode CSD–IBPRAC02) were used.

The results of calculations of the energetic terms of the (±)- and the (+)-IBP crystal lattices for both the **M** and the **G** force field are presented in Table 6. The van der Waals terms of both (+)- and (±)-IBP are approximately equal if calculated by the same force field. It should be noted that this value is slightly higher (absolute value) for the **G** force field than the analogous value for the **M** force field. In contrast, the terms connected to energies of hydrogen bonds show an opposite trend: for the **G** force fields, the term is $\sim$3 kJ · mol^{-1} less than that for the **M** force field. The opposite trends sum up to approximately the same total values of the crystal lattice energies obtained by the two force fields considered. It should be mentioned that for (±)-IBP, the ratio between the hydrogen bonding energy and the common crystal lattice energy is sensitive to the choice of the force field: 26.4% for the **G** force field and 32.3% for the **M**. The same tendency is observed for (+)-IBP: 24.9% for **G** and 29.7% for **M**. It should also be noted that the van der Waals term of (+)-IBP is higher (absolute value) than that of the (±)-IBP regardless of the force field used. Therefore, it may be assumed that for (±)-IBP, the loss of van der Waals energy [in comparison to (+)-IBP] is compensated by hydrogen bonding energy. Probably, these two energies are competing when enantiomer and/or racemate crystals are growing.

The value calculated for the crystal lattice energy of (+)-IBP is in a good agreement with the experimental data, within experimental errors. The analogous value for (±)-IBP is slightly lower compared to the experimental one. The data calculated here—although the separation into the various terms is very different—are in good agreement with data of Li et al.[4] as well (Table 6);

Table 6. Calculated Results of the Various Energetic Terms of (+)- and (±)-Ibuprofen Crystal Lattices Obtained by the Two Types of Force Fields[a] and Comparison with Analogous Literature Values[b,c]

Term[d]	(±)-IBP	(+)-IBP	Δ[(±) − (+)]	
Gavezzotti et al.[a]				
E^{vdw}	−78.0 (71.0)	−78.8 (72.8)	0.8	
E^{coul}_s	−2.8 (2.6)	−2.5 (2.3)	−0.3	
E^{HB}	−29.0 (26.4)	−26.9 (24.9)	−2.1	
E_{latt}	−109.8	−108.2	−1.6	
Mayo et al.[a]				Li et al.[b]
E^{vdw}	−71.7 (65.2)	−73.1 (68.2)	1.4	−11.0
E^{coul}_s	−2.8 (2.5)	−2.5 (2.1)	−0.3	2.7
E^{HB}	−35.5 (32.3)	−31.9 (29.7)	−3.6	0.4
E_{latt}	−110.0	−107.5	−2.5	−7.9
ΔH_{sub}	115.8 ± 0.6	107.4 ± 0.5	8.4	

[a] Mayo et al.[16] and Gavezzotti et al.[17]
[b] Li et al.[4]
[c] E^{term}/E_{latt} in % is presented in parentheses.
[d] Values exprssed in kJ · mol^{-1}.

that is, the racemate is more thermodynamically stable by 2.5 (**M**) and 7.9 kJ · mol^{-1}, respectively.

To analyze the contribution of different structural fragments of IBP to the packing, the molecule was divided into four fragments, as shown in Figure 1b. Then, the respective contribution to the common packing energy was calculated individually for each fragment (both as absolute and relative values). The results of the calculations are presented in Table 7 for the **M** force field. Because the two (+)-IBP molecules are situated in an asymmetric unit (A and B) of the crystal lattice, the matrix of interactions of the molecular fragments is not symmetric [in contrast to (±)-IBP, where the *S*- and *R*-enantiomers are connected by the symmetry center]. As evident from Table 7, only the difference of the location of the R_3 fragment in the A and B conformers essentially affects the redistribution of E^{vdw} between them.

Comparative analysis of the energetic terms of different types of nonbonded van der Waals interactions for the considered crystal lattices (Mayo et al.[16] force field, **M**) were carried out. The results tare presented in Figure 4. The dominating contributions for the both (+)- and (±)-IBP are the following interactions in order of importance: C–C > C–H > C–O. Moreover, a transition from (+)- to (±)-IBP makes the relative contributions of the C–H, C–C, and H–O terms decrease:, whereas the H–H, C–O, and O–O terms increase slightly.

Because C–H interactions for both compounds is >25% of the contribution to the common energy of the nonbonded van der Waals interactions, it should be expected that if the positions of the hydrogen atoms in the unit cells could be resolved more accurately by neutron diffraction experiments, the accuracy of the final result should be essentially increased. Shankland et al.[5] and Li et al.,[4] in particular, mentioned this fact. Lacking these data, we tried to estimate the influence of the C–H distance on the van der Waals term of the crystal lattice energy. For this purpose, in the calculation procedure, only the C–H distance was changed (from 0.95 to 1.20 Å), and the same coordinates of the other atoms in the unit cell were retained. The results of the calculation are presented in Figure 5. The solid symbols in Figure 5 denote the E^{vdw} values corresponding to the C–H bonds obtained from diffraction experiments. The

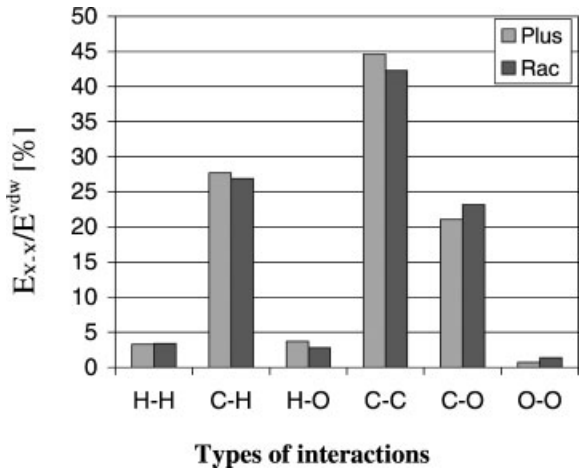

Figure 4. The energetic terms of different types of nonbonded van der Waals interactions of the (+)- and (±)-ibuprofen crystal lattices (Mayo et al.[16] force field).

Table 7. Calculated Results of the van der Waals Terms of the Packing Energy from the Various Fragments of Ibuprofen Molecule using the Mayo et al. Force Field[a]

(+)-IBP

Term[a]	R_1	R_2	R_3	R_4	Term[b]	R_1	R_2	R_3	R_4
R_1	−5.9	−6.7	−3.1	−3.5	R_1	8.1	9.2	4.3	4.8
R_2	−6.4	−5.9	−7.8	−6.3	R_2	8.7	8.0	10.6	8.6
R_3	−3.8	−4.6	−1.9	−2.4	R_3	5.2	6.2	3.3	3.2
R_4	−4.7	−5.4	−3.0	−0.2	R_4	6.4	7.4	5.4	0.3

(±)-IBP

Term[b]	R_1	R_2	R_3	R_4	Term[b]	R_1	R_2	R_3	R_4
R_1	−5.6				R_1	7.8			
R_2	−6.9	−6.3			R_2	9.6	8.8		
R_3	−1.8	−5.2	−2.4		R_3	2.5	7.2	3.4	
R_4	−3.1	−5.6	−5.0	−2.4	R_4	4.4	7.8	7.0	3.3

[a]Values expressed in kJ · mol^{-1}.
[b](E^{Ri-Rj}/E^{vdw}) 100% (%).

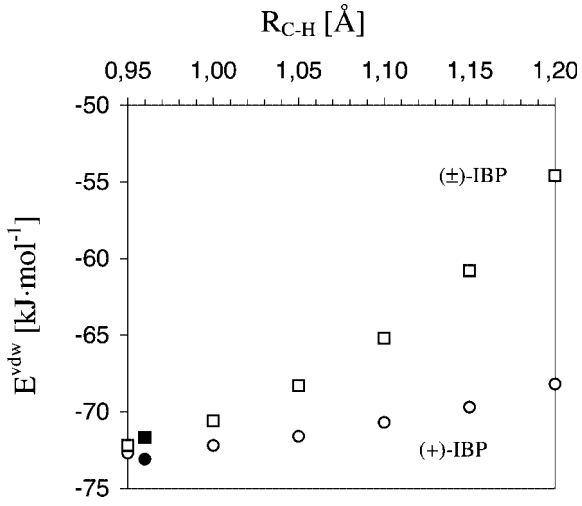

Figure 5. The dependence of the van der Waals term of the crystal lattice energy on the length of the C–H bond (the filled symbols mark the E^{vdw} values corresponding to the C–H bonds otained from the diffraction experiments).

results in Figure 5 indicate that within the noted variation interval of the C–H bond lengths, the E^{vdw} values are changed by 4.5 kJ · mol^{-1} for (+)-IBP and by 17.6 kJ · mol^{-1}for (±)-IBP. This fact confirms once more, that the van der Waals energy of the enantiomer is approximately two times less sensitive to C–H bond variations (6.2%) than is the racemate (24.4%). This fact also stresses that the estimation of crystal lattice energy for (+)-IBP does not depend too much on the accuracy of hydrogen atoms coordinates (by X-ray or neutron diffraction).

It should be noted that mathematical simulation of crystal lattice energies from X-ray data and comparison of the result with sublimation experiments is a classical approach. However, in the present work, sublimation experiments for racemate and enantiomer were carried out for the first time. Moreover, the particular value of the experimental part is that the experiments were carried out with the same method, under the same conditions, and with numerous data points. These conditions reduce the experimental errors to a minimum and allow the use of comparison procedures, which is particularly important for such kind of studies because differences between the thermodynamic functions of the sublimation process of racemates and the respective enantiomers (as a rule) are insignificant and, therefore, comparison analysis of the noted values is delicate. Another essential difference of the present work to studies devoted to the mathematical simulation of crystal lattice energies is the choice of functions to be compared. In numerous studies, the main focus is sublimation enthalpy, but in this work, all the thermodynamic functions (Gibbs energy, enthalpy, and entropy) were analyzed. This comprehensiveness is very important because knowledge of all these functions enables the prediction of driving forces of processes, such as resolution of enantiomers by crystallization, which are used for the preparation of pharmaceutical drug substances. Understanding the factors that control the formation of homochiral and racemate crystals may ultimately lead to the rationalization of the purification of enantiomers and the resolution of racemates by crystallization, respectively.

The transpiration method was used for sublimation studies of drugs by Griesser et al.[26] (caffeine). Experience indicates that the transpiration method is more effective than other sublimation methods (for example effusion method) because of a wider experimental temperature interval. This fact gives the opportunity (a) for more plausible interpretation of the collected data and (b) to work at lower temperature values in comparison with the traditional methods (reducing probability of compound decomposition).

CONCLUSIONS

In the present work, X-ray re-determination of the (+)-IBP crystal structure was carried out and the hydrogen bond geometry in the crystal lattice was solved. Attempts were made (using the Mayo et al.[16] and Gavezzotti[17] force fields) to compare (a) van der Waals and hydrogen bonding packing terms, (b) interactions of the various molecular fragments within the crystal lattice, and (c) the terms describing the different types of nonbonded interactions. The present approach gives the opportunity for a deeper understanding of the differences of drug–drug interactions in the crystal lattice of racemates and enantiomers, not only with respect to the energetic scale (ratio between specific and non specific interactions), but also with respect to thermodynamic parameters (Gibbs energies and entropic terms). This information is the basic knowledge needed for a rational development of the appropriate methods for the resolution of racemates to isolate the pure enantiomers (e.g., driving forces, temperature conditions, and minimal nuclei size of the crystallization technique).

ACKNOWLEDGMENTS

This work was generously supported by Norges Forskningsråd, project number HS 58101.

REFERENCES

1. Jamali F. 1993. Stereochemically pure drugs: An overview. In: Wainer IW, editor. Drug stereochemistry, 2nd edition. New York: Marcel Dekker, pp 275–284.
2. Wainer IW. 1993. Drug stereochemistry: Analytical methods and pharmacology, 2nd edition. New York: Marcel Dekker.
3. Brock CP, Schweizer WB, Dunitz JD. 1991. On the validity of Wallach's Rule: On the density and stability of racemic crystals compared with their chiral counterparts. J Am Chem Soc 113:9811–9820.
4. Li ZJ, Ojala WH, Grant DJW. 2001. Molecular modeling study of chiral drug crystals: Lattice energy calculations. J Pharm Sci 90:1523–1539.
5. Shankland N, Florence AJ, Cox PJ, Sheen DB, Love SW, Steward NS, Wilson CC. 1996. Crystal morphology of ibuprofen predicted from single-crystal pulsed neutron diffraction data. Chem Commun 7: 855–856.
6. Kimoto H, Saigo K, Hasegawa M. 1990. The potential energy calculation for conglomerate crystals. Chem Lett 5:711–714.
7. Leiserowitz L. 1976. Molecular packing modes. Carboxylic acids. Acta Crystallogr, Sect B 32:775–802.
8. Freer AA, Bunyan JM, Shankland N, Sheen DB. 1993. Structure of (*S*)-(+)-ibuprofen. Acta Crystallogr, Sect C 49:1378–1380.
9. McConnell JF. 1974. The 2-(4-isobutylphenyl) propionic acid. Ibuprofen or prufen. Cryst Struct Comm 3:73–75.
10. Shankland N, Wilson CC, Florence AJ, Cox PJ. 1997. Refinement of ibuprofen at 100 K by single-crystal pulsed neutron diffraction. Acta Crystallogr, Sect. C 53:951–954.
11. Ertel KD, Heasley RA, Koegel C, Chakrabarti A, Carstensen JT. 1990. Determination of ibuprofen vapor pressure at temperatures of pharmaceutical interest. J Pharm Sci 79(6):552.
12. Mura P, Bettinetti GP, Manderioli A, Faucci MT, Bramanti G, Sorrenti M. 1998. Interaction of ketoprofen and ibuprofen with β-cyclodextrins in solution and solid state. Int J Pharm 166:189–203.
13. Zielenkiewicz W, Perlovich G, Wszelaka-Rylik M. 1999. The vapor pressure and the enthalpy of sublimation determination by inert gas flow method. J Therm Anal Calorim 57:225–234.
14. Cox JD, Pilcher G. 1970. Thermochemistry of organic and organometallic compounds. London: Academic Press.
15. Kitaigorodsky AI. 1971. The molecular crystals. Moscow: Nauka.
16. Mayo SL, Olafson BD, Goddard WA III. 1990. Dreiding: A generic force field for molecular simulations. J Phys Chem 94:8897–8909.
17. Gavezzotti A, Filippini G. 1997. Energetic aspects of crystal packing: Experiment and computer simulations. In: Gavezzotti A, editor. Theoretical aspects and computer modeling of the molecular solid state. Chichester, UK: John Wiley & Sons, pp. 61–97, 237.
18. Perlovich GL, Kurkov SV, Bauer-Brandl A. 2003. Thermodynamics of solutions II: Flurbiprofen and diflunisal as models for studying solvation of drug substances. Eur J Pharm Sci 19:423–432.
19. Lebedev YA, Miroshnichenko EA. 1981. Thermochemistry of vaporization of organic substances. Moscow: Nauka, p 215.
20. Roimero AJ, Rhodes CT. 1993. Stereochemical aspects of the molecular pharmaceutics of ibuprofen. J Pharm Pharmacol 45:258–262.
21. Shankland N, Florence AJ, Cox PJ, Wilson CC, Shankland K. 1998. Conformational analysis of ibuprofen by crystallographic database searching and potential energy calculation. Int J Pharm 165: 107–116.
22. McArdle P. 1995. Computer program abstracts. J Appl Crystallogr 28:765.
23. Enraf-Nonius. 1989. *CAD-4 Software*. Version 5.0. Enraf-Nonius, Delft, The Netherlands.
24. Sheldrick GM. SHELXL97 and SHELXS97. 1997. University of Göttingen, Germany.
25. Adams SS, Bresloff P, Manson CG. 1976. Pharmacological differences between the optical isomers of ibuprofen: Evidence for metabolic inversion of ibuprofen. J Pharm Pharmacol 28:256–257.
26. Griesser UJ, Szelagiewicz M, Hofmeier UCh, Pitt C, Cianferani S. 1999. Vapor pressure and heat of sublimation of crystal polymorphs. J Therm Anal Calorim 57:45–60.
27. Evans AM. 2001. Comparative pharmacology of *S*(+)-ibuprofen and (*RS*)-ibuprofen. Clin Rheumatol 20(Suppl. 1):S9–S14.